engineering proceedings

MDPI

Proceeding Paper

An Effect of Coupling Factor on the Power Output for Electromagnetic Vibration Energy Harvester

Tunde Toluwaloju [1], ChungKet Thein [1,*] and Dunant Halim [2]

[1] School of Aerospace, University of Nottingham, Ningbo, China; Tunde.TOLUWALOJU@nottingham.edu.cn
[2] Department of Mechanical, Materials and Manufacturing Engineering University of Nottingham, Ningbo, China; Dunant.Halim@nottingham.edu.cn
* Correspondence: chungket.thein@nottingham.edu.cn
† Presented at 8th International Electronic Conference on Sensors and Applications, 1–15 November 2021; Available online: https://ecsa-8.sciforum.net.

Abstract: Sensors are devices that measures a change in physical stimulus by converting it into an electronic signal which can be read by a designated instrument. Notable sensing application include among others vibration sensing, temperature sensing, humidity sensing, strain sensing, biosensing and structural health monitoring (SHM). Powering SHM devices/sensors remotely and autonomously in a passive, efficient, ecofriendly means with minimum retrofitting cost has been a major desire over the past decades. A device that meets such specifications is the vibration energy harvester. This work focuses on the electromagnetic transduction harvester whose harvested voltage/power is formulated from Faraday law of electromagnetic induction. Electromagnetic parameter that determines the degree of transduction is referred to as the coupling constant. The value of coupling constant must be accurately set during harvester design because it directly determines the harvester damping ratio and power available for the sensor. In this work, we introduce an approach to effectively determine the harvester's optimum magnetic flux parameter that will be used in computing the optimum coupling constant, electromagnetic damping ratio and the power harvested at resonance. This work concludes that maximum power can be harvested for powering the sensor at certain optimum value of coupling value only. This optimum is attained by a tradeoff between the applied load resistance and resonant frequency. For designs considered here the resonant threshold is 20 Hz. Below this threshold, accumulated electromagnetic damping ratio becomes excessive. Also, the load resistance should be reasonably high to allow for optimum damping ratio during operation.

Keywords: vibration energy harvesting; coupling constant; flux density; coil fill factor; coil effective length

Citation: Toluwaloju, T.; Thein, C.; Halim, D. An Effect of Coupling Factor on the Power Output for Electromagnetic Vibration Energy Harvester. **2021**, *3*, x. https://doi.org/10.3390/xxxxx

Academic Editor(s):

Received: date
Accepted: date
Published: date

1. Introduction

Adequate study of structural dynamic characteristic is very important as a robust method for assuring the satisfactory integrity and health monitoring because an unpredicted failure may cause devastating consequences on economic, social, and human life. An example of SHM attempt is the cost-effective space division multiplexed hybrid vibration sensor used for vibration monitoring [1]. Most convectional sensors have shown limitations with their usage because they are mostly affected by electromagnetic interference and noise inclusion during analog/digital conversion [2]. Powering a SHM device with battery power module has some form of limitations to the continuously uninterrupted but cheap remote and autonomous operations [3]. A miniaturized and cost-effective power management system (PMS) for low-voltage electromagnetic energy harvesters (EMEHs) operating in both battery-powered and battery less applications was reported in [4]. A review [5] highlights the use of carbon nanomaterials as deposition materials for

fiber reinforcements using them as sensors for process monitoring during manufacturing and SHM during in-service life. An internet of things (IoT) based structural health monitoring using a customized data-logger with sensing nodes was a focus in [6]. The importance of railway in the transportation industry is steadily increasing although more than 35% of the 300,000 railway bridges across Europe are over 100-years old. SHM of railway bridges to evaluate their structural integrity directly impacts on the reliability of the railway networks [7]. Strategies employed to monitor bridge health against seismic and severe climatic actions has been discussed [8]. An analytical approach for quantifying the cost-benefit optimization using a stochastic methodology to optimally design structural health monitoring systems is proposed in [9].

A simple power module that has shown prospects to powering SHM devices/sensors remotely and autonomously is called an electromagnetic vibration energy harvester whose transduction depends on the electromagnetic coupling factor [11]. Four different methods of measuring the coupling constants were mentioned [12,13] and one of such methods is herein employed for this work. An investigation of the electro-mechanical coupling effect of a hybrid electromagnetic and piezoelectric energy harvester [14] reported that the bigger the coupling coefficient, the greater the resonant frequency shift, the output power, and the energy conversion efficiency. The effect of coupling strength on the efficiency of an electromagnetic energy harvester was shown in [15] concluding that, up to a certain point, increasing the coupling strength of the harvester substantially increases the output power, hence improving the device efficiency [15].

The focus in this work is on formulating an analytical equation for characterizing the harvester's optimum magnetic flux parameter to be used in computing the optimum coupling factor, the electromagnetic damping ratio, and the maximum resonant power.

2. Determination of the Harvester's Resonant Frequency

To properly define the harvester's resonant frequency, it is modelled as a fixed-free Single Degree of Freedom tip loaded beam as shown in Figure 1. The beam is modelled so that one end is fixed to a base. The transverse motion equation of the clamped-free cantilever beam excited in harmonic at base position x and time t can be described by the following equation.

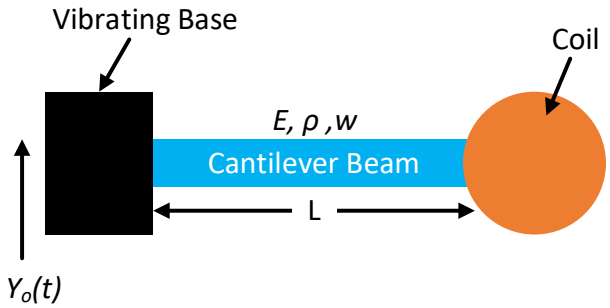

Figure 1. The vibration energy harvester modelled as a fixed-free SDOF cantilever beam with a tip coil mass fixed at its free end.

$$z_{abs}(x,t) = z_{rel}(x,t) + Y_0(t) \quad (1)$$

where $z_{abs}(x,t)$ is the absolute vertical beam displacement; $z_{rel}(x,t)$ is the vertical beam displacement relative to the fixed/clamped base; and $Y_0(t)$ is the vertical amplitude base excitation, h is thickness of beam, ρ is the density of the beam, w is the width of the beam, E is the young modulus of the beam and L is the length of the beam.

According to the Euler Bernoulli beam theory, the equation of motion that governs undamped free vibration of a beam is given as

$$\frac{EI}{\rho A}\frac{\partial^4 z_{rel}(x,t)}{\partial x^4} + \frac{\partial^2 z_{rel}(x,t)}{\partial t^2} = 0 \quad (2)$$

where E is the Young modulus, I is the second moment of area, ρ is the density, A is the cross-sectional area, and $EI$is the bending stiffness and ρA mass per unit length of the cantilever beam.

Considering each vibration mode n, the relative vertical beam displacement ($z_{rel}(x,t)$) for *n-th* mode can be represented as the product of the spatial (transverse displacement) and temporal (time) components. The Eigen equation associated with the mode shape and temporal response functions are described as follows:

$$\frac{d^4\varphi_n(x)}{dx^4} - {\lambda_n}^4\varphi_n(x) = 0 \quad (3)$$

$$\frac{d\eta_n(t)}{dt^2} + {\omega_n}^2\eta_n(t) = 0 \quad (4)$$

where $\eta_n(t)$ is the temporal response, $\varphi_n(x)$ is the mode shape response, ${\lambda_n}^4$ is the lumped parameter defined as $\frac{{\omega_n}^2\rho A}{EI}$; and ω_n is the *n-th* vibration mode's resonant frequency of the beam-mass system obtained as

$$\omega_n = \beta_n^2\sqrt{\frac{\mathrm{EI}}{\rho AL^4}} \quad (5)$$

Equation (5) shows that the resonant frequency could be obtained as a function of the harvester's geometry and properties.

3. Theoretical Determination of the Harvester Coupling Factor

From the harvester design standpoint, obtaining the accurate and precise electro-mechanical coupling in the harvester system is necessary for achieving maximum efficiency and highest harvestable power. According to the Faraday law of induction, the coupling constant (K) for the electromagnetic harvester can be expressed as

$$K = Nbc_f l_c \quad (6)$$

where b is the magnetic flux density; N is the number of the coil turn; c_f is the coil fill factor; and l_c is the effective length of the coil. For any coil design, the coupling Equation (6) considers three coil parameters, N, c_f and l_c, as fixed/non-variables while the parameter b is variable. These three parameters were considered fixed because it is peculiar to a specific coil design such that once the coil has been fabricated, it values cannot be altered.

The total damping ratio (ζ_T) of an electromagnetic vibration energy harvester had been reported as the sum of the mechanical damping ratio (ζ_{mech}) and the electromagnetic damping ratio (ζ_E) [13].

$$\zeta_T = \zeta_{mech} + \zeta_E \quad (7)$$

The mechanical damping is approximated using a method proposed by same author [13] where damping is related to the critically damped stress model. The electromagnetic damping (ζ_E) and the power harvested (P_{Coil}) in the coil winding is obtained using the Faraday law of induction for a circular coil geometry, is:

$$\zeta_E = \frac{8K^2{l_c}^2}{m_e\omega_n}\left(\frac{1}{R_l + R_c}\right) \quad (8)$$

$$P_{Coil} = 16K^2{l_c}^2(\omega_n z)^2\left(\frac{1}{R_l + R_c}\right) \quad (9)$$

where l_c is the effective coil length; m_e is the fundamental effective modal mass of the system; ω_n is the resonant frequency; R_l is the load resistance; and R_c is the coil resistance. Rearranging Equation (8) and making K as the subject of the formula:

$$K = \sqrt{m_e \omega_n \zeta_E \, (R_l + R_c) \left(\frac{1}{8 l_c^2}\right)} \tag{10}$$

Equations (8) and (10) show a direct dependency of the coupling factor on the electromagnetic damping ratio. The higher the electromagnetic damping ratio, the higher is the coupling factor. Hence to achieve the value of coupling that commensurate with any electromagnetic damping value, the value of b must then be sufficiently large enough.

It is sufficient to say that we could determine the optimum value of b by substituting the known coil parameters and resonant frequency value while setting $\zeta_E < 1$ into Equation (10). However, such a procedure will waste the effort because the power harvested and the electromagnetic damping ratio changes with the value of the load resistance.

4. Result and Discussion

As shown in Figure 2, the variation of damping for several resonant frequencies from 10 Hz to 50 Hz, is described.

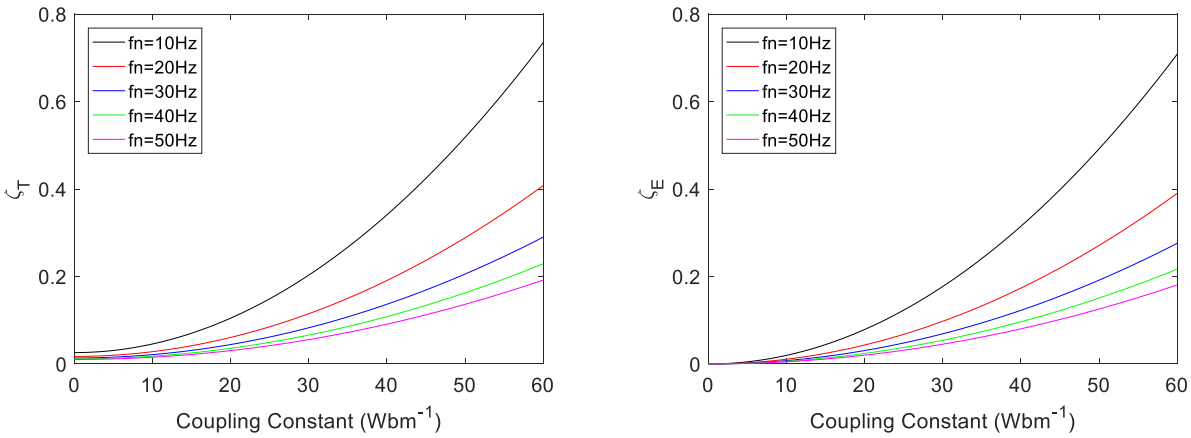

Figure 2. Comparison of the damping ratio with the coupling constant at different resonant frequencies for the total damping (**left**) and electromagnetic damping (**right**) when $R_l = 111.42\ \Omega$.

From Figure 2, the higher the resonant frequency, the lower is the damping but the coupling increases with an increased resonant frequency as in Equation (8). Based on a compromise between the degree of coupling and resonant frequency, there exists an optimum damping ratio at which the harvester performance becomes optimal, thereby maximizing the power harvested. The determination of the optimum damping ratio therefore becomes crucial because the power output would stagnate at a certain limit regardless of how high other electromagnetic parameters N, c_f and l_c become [13]. The approach adopted in this work is that using Equation (6), we plotted the damping ratio against the value of coupling until $60\ Wbm^{-1}$ over a range of flux density as shown in Figure 3. The figure shows the variation of the total damping ratio (left) with the coupling factor, and the variation of the electromagnetic damping ratio (right) with the coupling factor for the considered coil geometry having the following design parameters: $N = 800$ turns; $c_f = 0.7803$; $l_c = 79.671$ mm; and a load resistance $R_l = 111.42\ \Omega$.

The mechanical damping is reported as the sum of two independent damping components: material damping and thermoelastic damping [13–16]. The analysis shows that the mechanical damping ratio remains constant for any resonant frequency for all range

of the flux density considered and the magnitude is likewise independent on the value of the load resistance as shown in Figure 3.

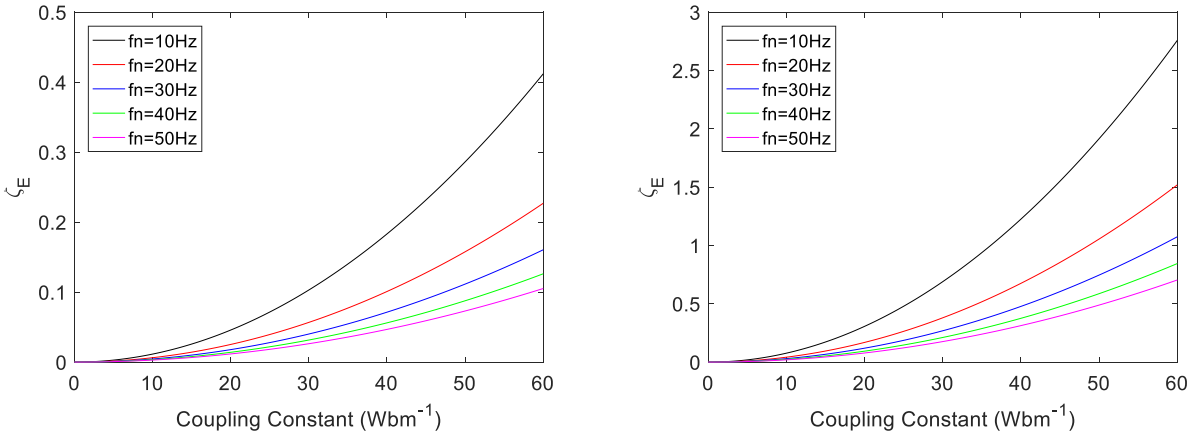

Figure 3. Comparison of the electromagnetic damping with the coupling constant at different resonant frequencies for different values of load resistance, $R_l = 200\ \Omega$ (**left**) and $R_l = 20\ \Omega$ (**right**).

These damping terms were reported to be frequency dependent but has no dependency on the load resistance thus explaining why the mechanical damping will not change with the load resistance. Since the mechanical damping remains constant and the same for each of the resonant frequency considered, the focus of further analysis will then be on the variation of the coupling

Figure 3 shows a comparison of the electromagnetic damping for different coupling factors using two values of load resistance, $R_l = 200\ \Omega$ (left) and $R_l = 20\ \Omega$ (right), at different resonant frequencies. The figure shows that the higher the load resistance, the lower is the damping ratio. In addition, the damping decreases as the resonant frequency increases. Intuitively we can then say that it is desirable to operate the harvester considered in this work in the frequency range above 20 Hz to avoid generating too large electromagnetic damping, which concurs with Equation (8).

Now we proceed to investigate how the electromagnetic damping-coupling plot varies with the load resistance. Figure 3 shows that for any specific resonant frequency, as the applied load increases, the electromagnetic damping ratio reduces. This observation confirms Equation (8) as the coupling factor increases, thus confirming the validity of Equation (10).

Figure 4 shows that there exists a point along the power-coupling factor curve where the harvested power becomes maximum for each specific resonant frequency. This maximized point is the location where the electromagnetic damping and the coupling factor becomes optimized, and each maximized resonant power peak corresponds to an optimized resonant value of the flux density which could be obtained using the optimum value of K and the coil parameters in described Equation (6).

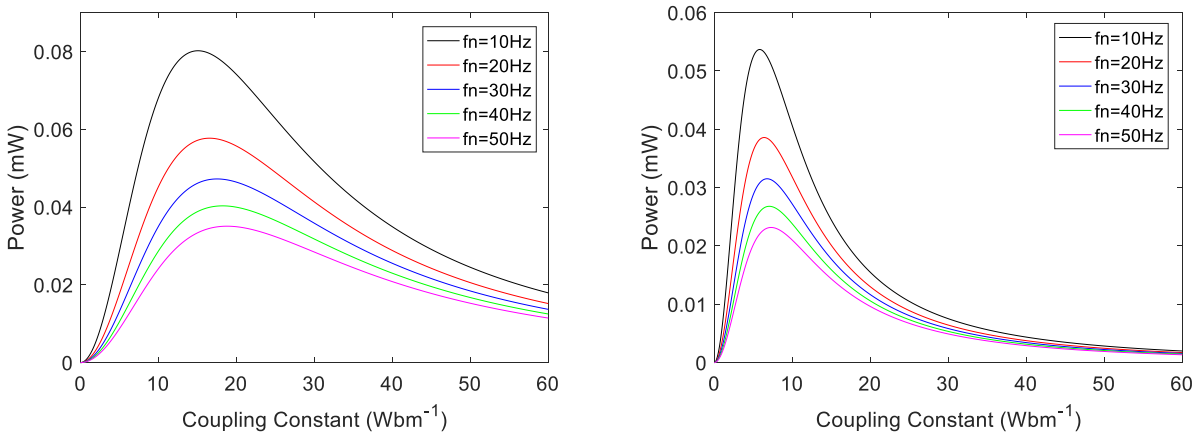

Figure 4. Power harvested against the coupling constant at different resonant frequencies for different values of load resistance, $R_l = 200\ \Omega$ (**left**) and $R_l = 20\ \Omega$ (**right**).

5. Conclusions

The work herein investigated the interdependency among the vibration energy harvester's coupling factor, the electromagnetic damping ratio harvested power and the load resistance. The analysis shows inverse dependence of the damping ratio with the load resistance thereby confirming Equation (8) while the harvested power as well as the coupling factor shows direct dependence to load resistance. This suggests that for any resonant frequency the harvested power harvested is maximized at certain optimum coupling factor for each resonant. Using the known coil parameters and the optimum resonant coupling factor in (6), we can then proceed to determine the optimum resonant flux density that will produce the maximum resonant power.

In summary, to ensure a higher harvested resonant power is available to the sensor node, the harvester must operate at certain threshold value (20 Hz in the design considered) and, the optimum resistance of the sensors must be made as reasonably high as possible to match the harvester's optimum resonant damping ratio used during the sensor fabrication.

Institutional Review Board Statement:

Informed Consent Statement:

Data Availability Statement:

References

1. Zhao, Z.; Tang, M.; Wang, L.; Guo, N.; Tam, H.-Y.; Lu, C. Distributed Vibration Sensor Based on Space-Division Multiplexed Reflectometer and Interferometer in Multicore Fiber. *J. Light. Technol.* **2018**, *36*, 5764–5772.
2. Richelli, A. EMI Susceptibility Issue in Analog Front-End for Sensor Applications. *J. Sensors* **2015**, *2016*, 1–9.
3. Wu, X.; Lee, D. Miniaturized piezoelectric energy harvester for battery-free portable electronics. *Int. J. Energy Res.* **2019**, *43*, 2402–2409.
4. Shousha, M.; Dinulovic, D.; Haug, M.; Petrovic, T.; Mahgoub, A. A Power Management System for Electromagnetic Energy Harvesters in Battery/Batteryless Applications. *IEEE J. Emerg. Sel. Top. Power Electron.* **2020**, *8*, 3644–3657.
5. Irfan, M.S.; Khan, T.; Hussain, T.; Liao, K.; Umer, R. Carbon coated piezoresistive fiber sensors: From process monitoring to structural health monitoring of composites–A review. *Compos. Part A. Appl. Sci. Manuf.* **2021**, *141*.
6. Muttillo, M.; Stornelli, V.; Alaggio, R.; Paolucci, R.; Di Battista, L.; de Rubeis, T.; Ferri, G. Structural health monitoring: An iot sensor system for structural damage indicator evaluation. *Sensors* **2020**, *20*, 1–15.
7. Vagnoli, M.; Remenyte-Prescott, R.; Andrews, J. Railway bridge structural health monitoring and fault detection: State-of-the-art methods and future challenges. *Struct. Health Monit.* **2018**, *17*, 971–1007.
8. Prendergast, L.J.; Limongelli, M.P.; Ademovic, N.; Anžlin, A.; Gavin, K.; Zanini, M. Structural Health Monitoring for Performance Assessment of Bridges under Flooding and Seismic Actions. *Struct. Eng. Int.* **2018**, *28*, 296–307.
9. Capellari, G.; Chatzi, E.; Mariani, S. Cost–benefit optimization of structural health monitoring sensor networks. *Sensors* **2018**, *18*, 2174.

10. Cepnik, C.; Radler, O.; Rosenbaum, S.; Ströhla, T.; Wallrabe, U. Effective optimization of electromagnetic energy harvesters through direct computation of the electromagnetic coupling. *Sensor's Actuators A. Phys*. **2011**, *167*, 416–421.
11. Mösch, M.; Fischerauer, G. A comparison of methods to measure the coupling coefficient of electromagnetic vibration energy harvesters. *Micromachines* **2019**, *10*, 826.
12. Foong, F.M.; Thein, C.K.; Yurchenko, D. A two-stage electromagnetic coupling and structural optimisation for vibration energy harvesters. *Smart Mater. Struct*. **2020**, *29*.
13. Mösch, M.; Fischerauer, G. A comparison of methods to measure the coupling coefficient of electromagnetic vibration energy harvesters. *Micromachines* **2019**, *10*, 826.
14. Challa, V.R.; Cheng, S.; Arnold, D.P. The role of coupling strength in the performance of electrodynamic vibrational energy harvesters. *Smart Mater. Struct.* **2012**, *22*, 25005.
15. Foong, F.M.; Thein, C.K.; Yurchenko, D. Important considerations in optimising the structural aspect of a SDOF electromagnetic vibration energy harvester. *J. Sound Vib*. **2020**, *482*, 115470.